J Clust Sci (2014) 25:1657–1664
DOI 10.1007/s10876-014-0764-7

ORIGINAL PAPER

Solvent-Free Synthesis of ZnO Nanoparticles by a Simple Thermal Decomposition Method

Mehdi Ranjbar · Mohammad Ali Taher · Abbas Sam

Received: 9 May 2014 / Published online: 26 July 2014

Abstract This paper reports on a novel processing route for producing ZnO nanoparticles by solid-state thermal decomposition of zinc(II) acetate nanostructures obtained by the sublimation of zinc(II) acetate powder. The sublimation process of the $Zn(OAc)_2$ powder was carried out in the temperature 150 °C for 2 h. In addition, nanoparticles of ZnO were obtained by solid-state thermal decomposition of the synthesized $Zn(OAc)_2$ nanostructures. The synthesized products were characterized by X-ray diffraction (XRD), scanning electron microscopy, transmission electron microscopy, photoluminescence spectroscopy, and energy dispersive X-ray spectroscopy. The sublimation process of the $Zn(OAc)_2$ powder was carried out within the range of 150–180 °C. The XRD studies indicated the production of pure hexagonal ZnO nanoparticles after thermal decomposition.

Keywords Nanoparticles · Oxidation · Zinc oxide · Photoluminescence · Thermal decomposition

M. Ranjbar (✉)
Young Researchers and Elite Club, Islamic Azad University, Kerman Branch, Kerman, Iran
e-mail: mehdi.ranjbar@outlook.com

M. A. Taher
Department of Chemistry, Shahid Bahonar University of Kerman, P.O. Box 76175-133, Kerman, Iran

A. Sam
Department of Mining Engineering, Faculty of Engineering, Shahid Bahonar University, Jomhouri Islami Blvd, P.O. Box 76169-133, Kerman, Iran

Introduction

Nanostructure materials have attracted much attention in the last few years due to their unique properties that are different from the bulk materials [1–3]. Zinc oxide is a material of particular interest because of its unique optical and electronic properties. Nanosized ZnO has great potentiality for being used in preparing solar cell [4] and gas sensors [5]. Transition metal chalcogenides, as unique combinations, have attracted much attention because of their special physical and chemical properties, and broad application in many fields. Recently, nano-scale chalcogenides are assuming great importance both in theory and in practice owing to their novel properties as a consequence of the large number of surface atoms and the three-dimensional confinement of the electrons [6]. These unique properties lead to appearance of new application, such as carbonylation [7], oxygen-lead selenide interaction [8], fabrication of diffractive optical elements [9], and synthesis of (Z)-tamoxifen [10]. The semiconducting ternary chalcogenides, AB_mC_n (A = Cu, Ag, Zn, Cd, etc.; B = Al, Ga, In; C = S, Se, Te, O) are also very attractive, due to their unique thermoelectric and photocatalytic properties [11–13]. One of them is ZnO, which has many different structures [14]. ZnO is a compound of zinc that exists in two forms, red zinc oxide and yellow zinc oxide. Use as a chemical intermediate for mercury salts, chlorine monoxide, antiseptic in pharmaceuticals, pigment and glass modifier, fungicide, preservative in cosmetics, formerly used in antifouling paints and as a material for cathodes for mercury batteries [15]. ZnO was the most unusual one in terms of its structural properties at ambient pressure, which are largely determined by the strong tendency for linear coordination of Zn to form the O–Zn–O chain geometry [14]. The structure of ZnO is built up of planar O–Zn–O zigzag chains lying in the *ac*-plane. The band gap of the ZnO at room temperature was measured to be 3.445 eV from the photoconductivity, and *n*-type electrical conductivity has been reported [16, 17]. In general, there are many effective methods for the preparation of transition metal chalcogenides such as microwave irradiation [18], hydrothermal [19], and solvothermal [20]. Among various techniques developed for the synthesis of metal chalcogenides, thermal decomposition is a novel method to produce stable monodispersed [21–23] and it is a rapidly developing research area. As compared to conventional method, it is much faster, cleaner and economical. However, an improvement in the thermal decomposition process should be made in preparing copper nanoparticles with controllable size and shape in order to extend the application areas and satisfy the needs of fundamental research. In this manuscript, the production method of ZnO nanoparticles is reported. One-dimensional (1D) nanostructures of zinc(II) acetate were synthesized by the sublimation process of $Zn(OAc)_2$ powder; then, ZnO nanostructures were prepared by solid-state thermal decomposition of the produced $Zn(CH_3COO)_2$ nanostructures. The utilized method has many advantages since it is a controllable, free solvent, template less, and economical method. The produced nanostructures were characterized by SEM, TEM, XRD, PL, and EDAX.

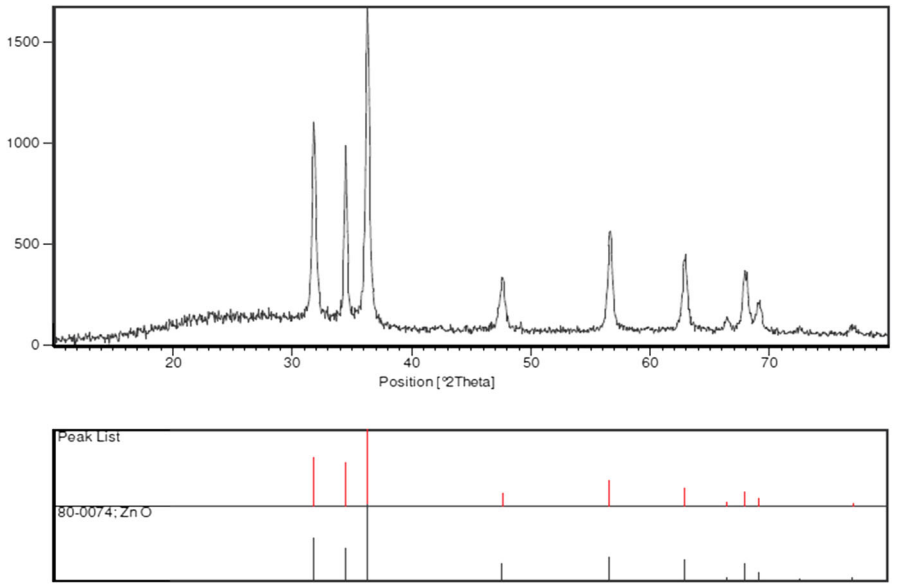

Fig. 1 XRD patterns of ZnO nanostructure sublimated at 350 °C

Experimental

Synthesis of $Zn(OAc)_2$ Nanostructures

In this work, zinc(II) acetate powder was used as the starting reagent. $Zn(OAc)_2$ nanostructures as precursor were prepared in a vertical quartz pipe set in vacuum condition. Each experiment was carried out by loading 1 g of zinc(II) acetate powder, which was transferred to the external pipe of the set. Then, the system was vacuumed by a pump. Afterwards, water entered the inner pipe from one side and exited from the other side. Water was circulated in the system in order to solidify the product vapors. The resulting product was gradually heated to the desirable temperature of 150 °C. After the heating process, the precipitations at the external part of the inner pipe were collected. The obtained products were characterized by SEM, and XRD.

Synthesis of ZnO Nanostructures

In a typical experiment, 1 g of the obtained $Zn(OAc)_2$ nanostructures was loaded into a silicon boat that was later put in a high-temperature tube furnace. The sample was heated in air at 350 °C for 120 min. After the thermal treatment, the system was allowed to cool to room temperature naturally, and the obtained precipitations were collected. The synthesized powders were characterized by SEM, TEM, XRD, Pl, and EDAX.

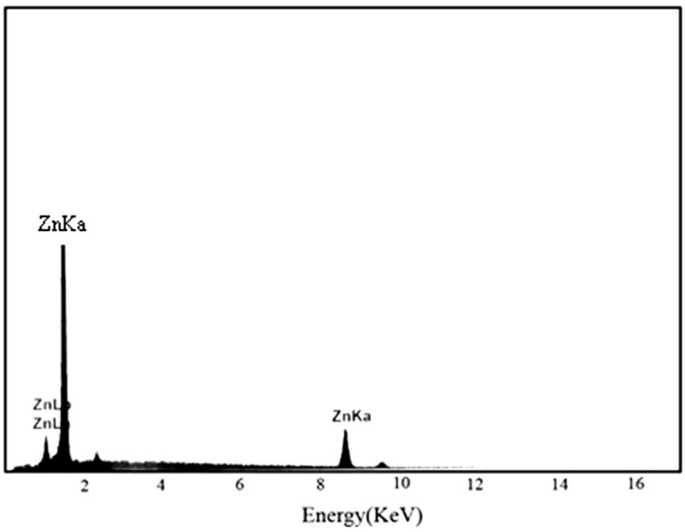

Fig. 2 EDAX pattern of ZnO

Results and Discussion

In recent years, there has been major interest in the amplification of coordination compounds for the synthesis of nanomaterials [18, 24]. Using new compounds can be highly useful since they can open new ways to prepare nanomaterials to control the shape and size distribution of nanostructures. In this work, $Zn(OAc)_2$ was applied as zinc precursor due to its high thermal stability and less reactivity toward nucleophilic agents than other organometallic precursors. XRD patterns ($10 < 2\Theta < 80$) of the synthesized $Zn(OAc)_2$ and ZnO are shown in Fig. 1a, b, respectively. The XRD pattern of the synthesized $Zn(OAc)_2$ at 150 °C (Fig. 1a) indicated the formation of monoclinic phase $Zn(OAc)_2$ (space group *P21/a*, JCPDS No. 031-0850). The XRD pattern of ZnO obtained from solid-state thermal decomposition of the synthesized $Zn(OAc)_2$ nanostructures at 350 °C is shown in Fig. 1b. Extremely broaden reflection peaks are observed in Fig. 1b, which indicates the fine nature of particles obtained from ZnO nanoparticles. All reflection peaks of the XRD pattern for ZnO nanoparticles are indexed well to hexagonal wurtzite phase of ZnO (space group: *Imm2*; JCPDS No. 80-0074) with calculated cell parameters a = 3.3110 A and b = 5.5260 Å. Based on XRD data, the crystallite diameter (D_c) of ZnO nanoparticles was calculated as 35 nm using the Scherer equation [18]:

$$D_c = K\lambda/\beta\cos\theta \quad \text{Scherer equation}$$

where β is the breadth of the observed diffraction line at its half intensity maximum, K is the so-called shape factor, which usually takes a value of about 0.9, and λ is the wavelength of X-ray source used in XRD. EDAX analysis was employed to investigate the chemical composition and purity of the synthesized ZnO

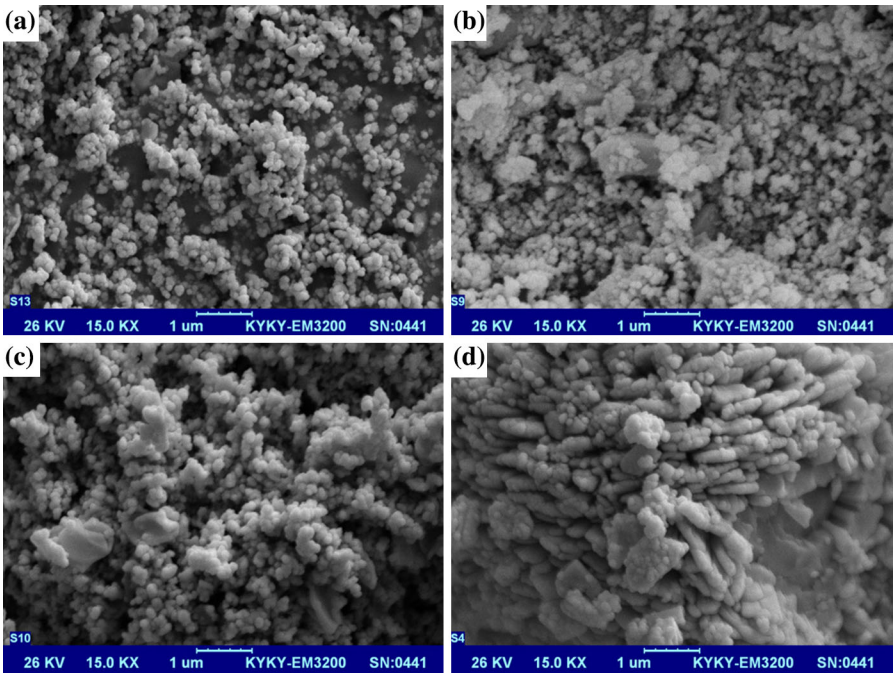

Fig. 3 SEM images of the $Zn(OAc)_2$ sublimated at **a** 150, **b** 160, **c** 170, **d** 180 °C

nanoparticles. A typical EDAX spectrum of ZnO nanoparticles, as shown in Fig. 2, indicates the presence of Zn in the product. In addition, neither N nor C signals were detected in EDAX spectrum. Therefore, both XRD and EDAX analyses show that pure ZnO nanoparticles are successfully produced via the mention synthetic route. In the present research, the effect of the thermal decomposition temperature on the morphology of $Zn(OAc)_2$ nanoparticles with a fixed reaction time of 2 h was investigated by SEM. SEM images of samples 1–4 were prepared at 150, 160, 170, and 180 °C, and called as samples A, B, C, and D, respectively. Figure 3a–d illustrates SEM images of the $Zn(OAc)_2$ sublimated within the range of 150–180 °C. The morphology of all samples is particle-like; however, by increasing the reaction temperature from 150 to 180 °C, the particle size of the products increased. To synthesize ZnO nanoparticles, the produced $Zn(OAc)_2$ nanoparticles were used as precursor. SEM image of the ZnO nanoparticles was created through solid-state thermal decomposition process of the $Zn(OAc)_2$ as shown in Fig. 4b. The formation of nanoparticles with an average size of 50 nm is seen in Fig. 4b. To further investigate the details of morphology, we took TEM image from the sample. From the SEM image displayed in Fig. 4b, we can find that the ZnO nanoparticles aggregated to some extent, although 20 min of sonication was employed in order to disperse it before the sample was deposited on the carbon coated copper grid for the TEM measurement.TEM image of ZnO nanoparticles is shown in Fig. 4a. The ZnO nanostructure consists of separated sphere-like nanostructures with particle size of

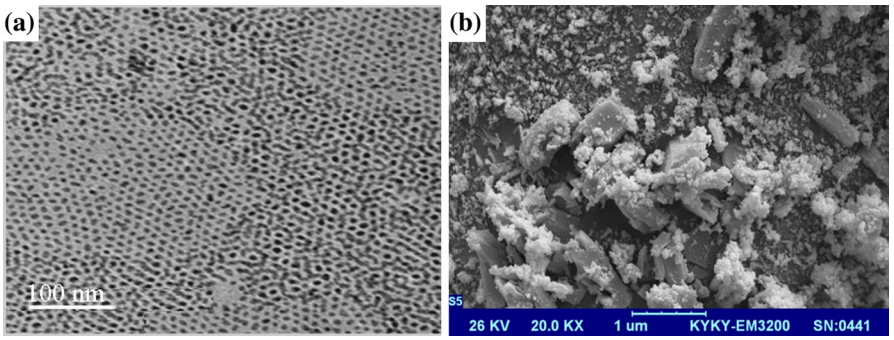

Fig. 4 **a** TEM image, and **b** SEM image of the ZnO nanoparticles synthesized from the $Zn(OAc)_2$ sublimated at 150 °C as precursor

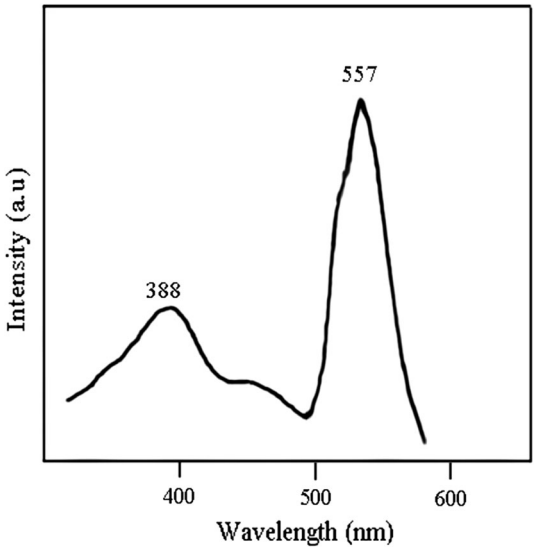

Fig. 5 Room temperature PL spectra of ZnO excited at 220 nm

~30 nm, almost consistent with what observed from SEM image of ZnO nanoparticles. Room temperature PL spectrum of ZnO nanoparticles excited at 220 nm is presented in Fig. 5. The PL spectrum (Fig. 5) shows two emission bands at about 388 and 557 nm. A emission band above 557 can be related to a singly charged oxygen vacancy, which results from the recombination of a photo generated hole with a charge state of the specific defect, such as oxygen vacancies, or resulted from the surface deep-level [25]. By using photoluminescence spectra, band gap can be determined along with the relative energetic position of sub-band gap defect states [26].This method can be developed to synthesize various metal oxides. By comparing this method and other works [27], it was found that the present method is a simple, fast, and cost-effective.

Conclusions

For the first time, ZnO nanoparticles have been successfully synthesized through a solid-state thermal decomposition method. We investigated the influence of the thermal decomposition temperature on the morphology of ZnO nanoparticles. The characteristics of products were determined by using XRD, SEM, PL, EDAX, and TEM analysis. The XRD results indicated that pure ZnO nanoparticles without any impurities could be obtained after thermal decomposition at 350 °C for 2 h. Finally, SEM results indicated that by increasing reaction temperature, the particle size of ZnO nanoparticles increased.

Acknowledgments Authors are grateful to council of University of Shahid Bahonar Kerman and Gol-E-Gohar Iron Mine for supporting this work.

References

1. S. M. Hosseinpour-Mashkani and M. Ramezani (2014). *Mater. Lett.* **130**, 259–262.
2. S. M. Hosseinpour-Mashkani, M. Ramezani, and M. Vatanparast (2014). *Mater. Sci. Semicond. Process.* **26**, 112–118.
3. S. M. Hosseinpour-Mashkani, K. Venkateswara Rao, Z Chamanzadeh, *International Conference on Nanoscience Engineering and Technology ICONSET* (IEEE¸ 2011), pp. 653–655.
4. K. Westermark, H. Rensmo, T. A. C. Lees, J. G. Vos, and H. T. Siegbahn (2002). *J. Phys. Chem. B.* **10**, 10108–10113.
5. H. M. Lin, S. J. Tzeng, P. J. Hsiau, and W. L. Tsai (1998). *Nanostruct. Mater.* **10**, 465–477.
6. M. Nanu, J. Schoonman, and A. Goossens (2012). *Nano Lett.* **5**, 1716–1720.
7. I. Tsuji, H. Kato, and A. Kudo (2011). *Angew. Chem. Int. Ed.* **44**, 356–361.
8. S. M. Hosseinpour-Mashkani, F. Mohandes, M. Salavati-Niasari, and K. Venkateswara-Rao (2012). *Mater. Res. Bull.* **47**, 314–319.
9. S. M. Hosseinpour-Mashkani, K. Venkateswara-Rao, and Z. Chamanzadeh (2011). *IEEE ICONSET* **47**, 653–659.
10. W. Zhou, Z. Yin, D. H. Sim, H. Zhang, J. Ma, H. H. Hng, and Q. Yan (2011). *Nanotechnology* **22**, 195–199.
11. M. L. A. Aguilera, M. Ortega-Lopez, V. M. S. Resendiz, J. A. Hernandez, and M. A. G. Trujillo (2003). *Mater. Sci. Eng. B* **102**, 380–385.
12. K. Yoshino, H. Komaki, T. Kakeno, Y. Akaki, and T. Ikari (2003). *J. Phys. Chem. Solids* **64**, 183–189.
13. S. Shen, L. Zhao, and L. Guo (2011). *Mater. Res. Bull.* **44**, 100–105.
14. F. Soofivand, M. Salavati-Niasari, and F. Mohandes (2012). *Micro. Nano. Lett.* **7**, 283–289.
15. L. Andronic, L. Isac, A. Duta, and J. Photoch (2011). *Photobiology A* **221**, 30–36.
16. M. Mousavi-Kamazani, M. Salavati-Niasari, and H. Emadi (2012). *Mater. Res. Bull.* **47**, 398–401.
17. M. Mousavi-Kamazani, M. Salavati-Niasari, and H. Emadi (2012). *Micro. Nano. Lett.* **7**, 896–901.
18. H. Kim, M. Suh, B. H. Kwon, D. S. Jang, S. W. Kim, and D. Y. Jeon (2011). *J. Colloid Interface Sci.* **363**, 703–708.
19. D. C. Pan, L. J. An, Z. M. Sun, W. Hou, Y. Yang, Z. Z. Yang, and Y. F. Lu (2008). *J. Am. Chem. Soc.* **130**, 562–569.
20. M. Salavati-Niasari, J. Javidi, and F. Davar (2010). *Ultrason. Sonochem.* **17**, 870–877.
21. Y. Akaki, S. Kurihara, M. Shirahama, K. Tsurugida, S. Seto, T. Kakeno, and K. Yoshino (2005). *J. Phys. Chem. Solids* **66**, 185–189.
22. I. Tsuji, H. Kato, and A. Kudo (2011). *Chem. Mater.* **18**, 196–200.
23. M. Ortega-Lopez, O. Vigil-Galan, F. C. Gandarilla, and O. Solorza-Feria (2003). *Mater. Res. Bull.* **38**, 55–61.

24. Z. Aissa, A. Bouzidi, and M. Amlouk (2010). *J. Alloys Compd.* **506**, 492–496.
25. M. Salavati-Niasari, N. Mir, and F. Davar (2009). *J. Alloys Compd.* **476**, 908–912.
26. L. Tian and J. J. Vittal (2007). *New J. Chem.* **31**, 208–211.
27. M. L. A. Aguilera, J. R. A. Hernandez, M. A. G. Trujillo, M. O. Lopez, and G. C. Puente (2007). *Thin Solid Films* **515**, 627–630.